HHS Public Access

Author manuscript

Vision Res. Author manuscript; available in PMC 2019 November 01.

Published in final edited form as:

Vision Res. 2018 November ; 152: 101–109. doi:10.1016/j.visres.2017.08.008.

Perceptual learning induces changes in early and late visual evoked potentials

Maryam Ahmadi[1], **Elizabeth A. McDevitt**[1], **Michael A. Silver**[2,3,4], and **Sara C. Mednick**[1]

[1]Department of Psychology, UC Riverside

[2]Helen Wills Neuroscience Institute, UC Berkeley

[3]School of Optometry, UC Berkeley

[4]Vision Science Graduate Group, UC Berkeley

Abstract

Studies of visual cortical responses following visual perceptual learning (VPL) have produced diverse results, revealing neural changes in early and/or higher-level visual cortex as well as changes in regions responsible for higher cognitive processes such as attentional control. In this study, we investigated substrates of VPL in the human brain by recording visual evoked potentials with high-density electroencephalography (hdEEG) before (Session 1) and after (Session 2) training on a texture discrimination task (TDT), with two full nights of sleep between sessions. We studied the following event-related potential (ERP) components: C1 (early sensory processing), P1 and N1 (later sensory processing, modulated by top-down spatial attention), and P3 (cognitive processing). Our results showed a significant decrease in C1 amplitude at Session 2 relative to Session 1 that was positively correlated with the magnitude of improvement in behavioral performance. Although we observed no significant changes in P1 amplitude with VPL, both N1 amplitude and latency were significantly decreased in Session 2. Moreover, the difference in N1 latency between Session 1 and Session 2 was negatively correlated with behavioral improvement. We also found a significant increase in P3 amplitude following training. Our results suggest that VPL of the TDT task may be due to plasticity in early visual cortical areas as well as changes in top-down attentional control and cognitive processing.

Keywords

Visual Perceptual Learning; Electroencephalogram; Event-Related Potentials; Texture Discrimination

Corresponding author: Maryam Ahmadi, Department of Psychology, UC Riverside, 900 University Ave, Riverside, CA 92521, mahmadi@ucr.edu.

1. Introduction

Visual perceptual learning (VPL) refers to the long-term improvement in perception of a visual stimulus with practice. Depending on the training characteristics, VPL can be specific to the features of the trained stimulus, meaning that behavioral improvements do not transfer to untrained stimulus features (Hung and Seitz, 2014; Karni and Sagi, 1991, 1993; Zhang et al., 2015). For instance, training improves performance on a texture discrimination task (TDT) (Karni and Sagi, 1991; 1993) that involves discriminating the orientation of a set of three diagonal bars that are arranged either horizontally or vertically and embedded within a background of horizontally or vertically oriented elements. This improvement in performance is long-lasting and specific to the trained stimulus: changing either the target location or the orientation of the background elements after training caused performance to return to pre-training levels (Karni and Sagi, 1991; 1993; Stickgold, James and Hobson, 2000).

Based on the location and orientation specificity of these training effects, it has been suggested that perceptual learning of TDT is due to plasticity in primary visual cortex (V1). Plasticity in sensory cortical areas following VPL has also been observed in multiple electrophysiological and neuroimaging studies (Bao et al., 2010; Furmanski, Schluppeck, and Engel, 2004; Pourtois et al., 2008; Schwartz, Maquet and Frith, 2002; Seitz and Watanabe, 2005; Sigman et al., 2005; Walker et al., 2005; Yotsumoto et al., 2008). However, other studies of VPL have suggested involvement of higher visual areas (Dosher and Lu, 1998; Petrov et al., 2005; Raiguel et al., 2006; Song et al., 2005; Yang and Maunsell, 2004) and in higher-order cortical regions such as prefrontal cortex (Wang et al., 2016). In macaque monkeys, perceptual learning induced changes in area V4 (Yang and Maunsell, 2004), an intermediate level of the visual cortical processing hierarchy, that were greater than those observed in V1 (Raiguel et al., 2006). Dosher and Lu (1998) proposed a model that describes VPL as a task-specific reweighting of the connections between visual processing areas and decision units. In this model, plasticity in early visual cortex is not necessary for VPL to result in behavioral improvements (Dosher and Lu, 1998; Petrov et al., 2005).

Studies of event-related potentials (ERPs) following VPL of TDT have produced mixed results regarding modulation of the C1 component, an early visual evoked potential thought to mainly reflect responses in primary visual cortex (V1) (Clark, Fan and Hilyard, 1995; Di Russo et al., 2001; Jeffreys and Axford, 1972), as well as later ERP components related to attention and decision making (Pourtois et al., 2008; Qu et al., 2014; Wang et al., 2016). Pourtois et al. (2008) reported decreased C1 amplitude after extensive training on the TDT. However, others found no effect of TDT training on C1 amplitude but significant neural changes in components related to higher-order cortical processes such as frontal P2, posterior P1, posterior P160-350, and anterior P160-350 (Qu et al., 2014; Wang et al., 2016).

Here we analyzed ERP responses of early (C1) and late (P1 & N1) visual evoked potentials as well as responses related to higher-order cognition (P3). The P1 and N1 components are sensory evoked potentials that peak within the first 200 ms of stimulus processing, with P1 normally observed around 100 ms, and N1 150–200 ms, after stimulus onset. A large body

of literature has shown modulation of P1 and N1 components by visual spatial attention (Hillyard and Anllo-Vento, 1998; Luck et al., 1994; Luck et al., 2000; Mangun et al., 1995; Noesselt et al., 2002; Rugg et al., 1987; Van Voorhis and Hillyard, 1977). C1, P1, and N1 are exogenous ERP components, meaning that their amplitudes and latencies are primarily a function of the physical properties of external stimuli. We also studied the P3 component, an endogenous component that peaks approximately 300 ms after stimulus onset over the parietal cortex. Unlike exogenous components, P3 is not modulated by the physical properties of external stimuli, but it is strongly modulated by attention, arousal level, memory processing, and decision-making (Hruby and Marsalek, 2003; Linden, 2005; Polich, 2007; Polich and Kok, 1995; Sutton et al., 1965).

Simultaneous measurement of C1, N1, P1, and P3 components allowed us to characterize the effects of VPL of TDT on electrophysiological signals at multiple levels. Changes in the amplitude and/or latency of the C1 component would suggest a contribution of primary visual cortical area V1 to VPL. Additionally, if training on the TDT changes attentional demands, this could result in altered P1 and/or N1 components. Finally, changes in the P3 component would suggest involvement of higher-order cortical processes such as decision-making.

In this study, we recorded hdEEG while participants performed the TDT both before training (Session 1) and 48 hours after training (Session 2). Given the ongoing debate about the neural mechanisms underlying VPL, our main goal was to assess the effects of VPL on early and late ERP components associated with primary visual cortex and/or higher-order cortical areas, respectively.

2. Methods

2.1. EEG recordings

EEG data were acquired using a 64-channel cap (EASEYCAP GmbH) with Ag/AgCI electrodes placed according to the international 10–20 System (Jasper, 1958). Fifty-six out of 64 electrodes were active scalp recordings. The remaining electrodes were the following: two electrocardiogram (ECG), two electromyogram (EMG), two electrooculogram (EOG), 1 ground, and 1 on-line common reference channel (at FCz location, retained after re-referencing). EEG signals were recorded at a 1000 Hz sampling rate and referenced on-line to the common reference channel.

After recording, EEG data from electrodes with impedance more than 3KΩ (on average, 8% of electrodes) were replaced with interpolation using the EEGLAB Toolbox (Delorme and Makeig, 2004). Next, EEG signals were re-referenced to the average of all active scalp electrodes and filtered between 0.05 to 40 Hz. Epochs were extracted from 200 ms before stimulus onset to 500 ms after stimulus onset and were baseline corrected over the 200 ms pre-stimulus interval. Trials with incorrect behavioral responses and those contaminated by movement artifacts, eye blinks, and/or eye movements exceeding ±50 uV were excluded from further analysis.

2.2. Subjects

Twenty healthy, non-smoking adults between the ages of 18 and 35, with no personal history of neurological, psychological, or other chronic illness gave informed consent to participate in the study. The Western Institutional Review Board approved all experimental procedures in accordance with the code of Ethics of the World Medical Association (Declaration of Helsinki).

Subjects were asked to maintain a consistent sleep-wake schedule during the week prior to and throughout the experiment, which included going to bed no later than 1:30 AM, waking up no later than 9:30 AM, and spending at least 8 hours in bed each night. Subjects were also asked to refrain from consuming caffeine, alcohol, and all stimulants for 24 hours prior to and including each study day. Heavy caffeine users (>240 mg per day) were also excluded to minimize the possibility of significant withdrawal symptoms during the experiment. Subjects completed sleep diaries and wore actigraph wrist monitors (Actiwatch Spectrum, Respironics) during the entire week prior to the experiment to provide subjective and objective measures of sleep-wake activity, respectively.

2.3. Stimulus and task

Subjects performed a version of the TDT that was adapted from Karni and Sagi (1991). Visual stimuli for the TDT were created using the Psychophysics Toolbox (Brainard, 1997; Kleiner et al., 2007; Pelli, 1997). Each stimulus contained two targets: a central letter (‘T’ or ‘L’), and a peripheral array of three diagonal line segments in either the upper right or upper left quadrant at 2.5°–5.9° eccentricity from the center of the display. The three line segments in the peripheral array were arranged either horizontally or vertically within a background of horizontally- or vertically-oriented background elements, resulting in a texture (line segment orientation) difference between the target and the background (Figure 1a).

An experimental trial consisted of the following sequence: central fixation cross for 600 ms, blank screen for 300 ms, target screen for 17 ms, blank screen (the inter-stimulus-interval, or ISI: variable duration with range 50–400 ms), mask for 100 ms, response interval for 2 s, and feedback (red fixation cross for incorrect trials and green fixation cross for correct trials) for 250 ms. The next trial started after 1500 ms of presentation of a blank screen. Subjects made two key presses to report both the central (letter identity; ‘T’ or ‘L’) and peripheral (orientation of three diagonal lines; horizontal or vertical) target identity on each trial.

In each session, subjects completed multiple runs of the TDT. In the first run, the ISI was fixed at 500 ms (Pourtois et al., 2008; Wang et al., 2016), and subjects completed 7 blocks of 15 trials each (total of 105 trials). In the second run (10 blocks of 15 trials, 150 trials total), a method of constant stimuli was employed, with a progressively shorter ISI (the specific sequence of ISIs was 400, 300, 250, 200, 167, 150, 134, 117, 100, and 50 ms). For this run, percent correct trials as a function of ISI was fit with a Weibull function to estimate a behavioral threshold (the ISI at which performance yielded 80% accuracy).

In Session 2, there was also a third run (same sequence of ISIs as in the second run, 10 blocks of 15 trials, 150 trials total) with a background orientation that was orthogonal to the background used during training and had never been previously seen by the subjects.

Session 2 always started with the fixed 500 ms ISI run, followed by the two runs with progressively shorter ISIs in each block. One of these latter two runs had the trained background orientation, and the other had the untrained background orientation. The order of these runs (trained versus untrained background) was counterbalanced across subjects.

EEG data were recorded during all runs, but only the EEG data from the first run (with fixed 500 ms ISI) of each session are analyzed here (the brief ISIs used for the trials used to obtain behavioral thresholds make it difficult to separate ERPs in response to the target array and to the mask). For all runs, subjects were able to control the time of onset of each block and were instructed to take as many breaks as needed between blocks.

A chin rest was adjusted to position each subject 60 cm from the stimulus presentation screen. Subjects were randomly assigned a specific stimulus condition for training (target location in either the upper left or upper right quadrant; background element orientation either vertical or horizontal) and practiced the task in this condition before starting the first run. Once subjects were at least 90% correct for peripheral target discrimination, they proceeded to the experimental runs.

2.4. Experimental timeline

Figure 1b illustrates the experimental timeline for this experiment. The data reported here are from the placebo sessions of a larger pharmacological study. At 9 AM on Day 1, subjects began Session 1, which included two runs of the TDT task - the first run yielded the EEG data used for ERP analysis, and the second run yielded the behavioral data used to estimate performance thresholds. Subjects then had two nights of sleep and returned to the lab 48 hours later on Day 3 to complete Session 2. This session included three runs of the TDT – the first run for ERP data, and the second and third runs to estimate thresholds for the trained and untrained stimulus conditions.

2.5. Data Analysis

2.5.1. Behavioral—TDT thresholds were compared between Session 1 and Session 2 using repeated-measures analysis of variance (ANOVA). To examine the magnitude of perceptual learning, we computed the performance difference score between Session 1 and 2 thresholds for each condition; positive values indicate lower thresholds (task improvement) following training.

2.5.2. ERP Analysis—Grand average ERP responses to the TDT target presentation were computed, and four distinct ERP components were identified based on their distinctive polarities, latencies and topographic maps: C1, P1, N1, and P3. C1 polarity is a function of visual field location of the stimulus – it is generally positive when the target is presented in the lower visual field and negative when it appears in the upper visual field, consistent with neural generators on either side of the calcarine sulcus in cortical area V1 (Di Russo et al., 2003). In the current study, visual stimuli were always presented in the upper visual field, resulting in a C1 component with a negative peak for all subjects and conditions.

We quantified amplitudes of C1, P1, N1 and P3 as the mean value between 45–90, 80–130, 125–190, and 220–500 ms after stimulus onset, respectively. Latencies were defined as the

time following stimulus onset at which a given component reached its maximum/minimum peak.

For each ERP component, electrode sites with prominent scalp activity were selected for analysis. The C1 component was assessed at CPz, Pz, and POz sites; the P1 component at P1, Pz, and P2; the N1 component at P3, P5, P7, PO3, O1, P4, P6, P8, PO4, and O2; and the P3 component at P1, Pz, and P2. Repeated-measures ANOVAs were used to examine mean amplitudes and peak latencies for each ERP component, with factors of Session (1 or 2), electrode site (see above), and hemisphere (ipsilateral or contralateral to the peripheral target stimulus location). Post-hoc pairwise t-tests were conducted to further characterize significant main effects from the ANOVAs.

Furthermore, changes in mean amplitude and peak latencies of each ERP component for each subject were correlated with performance difference scores. For each ERP measure, we performed an outlier test with a threshold of 2.5 standard deviations from the mean, and no data were excluded from the correlation analyses based on this criterion.

2.5.3. Analysis of Latency-Corrected Averages—To further study learning-induced changes in ERP components, we minimized the variability due to inter-trial fluctuations in latency of ERP components by computing latency-corrected averages. Specifically, we shifted each single-trial time series in time so that the latency of a selected ERP component matched that of the time series averaged across trials (Navajas, Ahmadi and Quian Quiroga, 2013; Quian Quiroga et al., 2007; Ray et al., 2015). We used a wavelet-based denoising algorithm to more effectively extract single-trial ERPs (Ahmadi and Quian Quiroga (2013) and used the latency of these single-trial ERPs to compute latency-corrected averages.

2.5.3.1. Single-trial ERP Denoising: Average ERPs were decomposed into six frequency bands using multiresolution decomposition. Wavelet coefficients related to the average ERP components were first selected automatically (Ahmadi & Quian Quiroga, 2013) and then further refined manually (Quian Quiroga, 2000; Quian Quiroga and Garcia, 2003). Next, the values of the coefficients that were unrelated to the average ERP components were set to zero (hard thresholding), as in Ahmadi and Quian Quiroga (2013).

Denoising of both the average and single-trial ERPs was carried out by applying the inverse wavelet transform, using the set of selected coefficients from Session 1 for a representative subject, to reconstruct the time series for both Session 1 and Session 2 for all the subjects (Navajas, Ahmadi and Quian Quiroga, 2013). By removing the contribution of unrelated coefficients, this method improves the estimation of peak amplitude and latencies of single-trial ERP components, compared with non-denoised data (Ahmadi and Quian Quiroga, 2013; Quian Quiroga, 2000; Quian Quiroga and Garcia, 2003).

2.5.3.2. Latency-corrected Averages: Next, we latency corrected single trials in denoised data to assess whether the learning-induced changes in N1 amplitude were a direct consequence of changes in C1 or P3 amplitude (there were no learning-induced changes in P1). For each subject, the extracted single-trial N1 components were aligned to the average N1 response for that subject, and then the latency-corrected grand average ERP was

calculated by averaging the latency-corrected averages for each subject. Aligning N1 in this way increases (negatively) the N1 amplitude, and we determined the effect of this N1 latency correction on C1 and P3 amplitudes. If increasing N1 amplitude through latency correction did not increase C1 amplitude, we could conclude that the learning-induced changes in N1 are not a direct consequence of changes in C1. Similar considerations apply to possible relationships between the N1 and P3 components.

We also performed latency correction on C1 and measured its effects on the amplitudes of the other ERP components. The sign test (Conover, 1999) was used to test for statistical significance of the difference between each component before and after latency correction.

3. Results

3.1. Behavioral results

Figure 2 displays behavioral thresholds for TDT for both Session 1 and Session 2. Behavioral effects of learning were assessed using paired t-tests. There was a significant decrease in threshold between sessions for the trained background ($p = 0.012$), indicating that VPL occurred with training. The threshold for the untrained background was significantly greater than that of the trained background in Session 2 ($p = 0.02$), but it was no different than that the trained background in Session 1 ($p = 0.56$), indicating that TDT VPL was specific to the orientation of the background elements. Moreover, average behavioral TDT performance for the 500 ms ISI trials used for the ERP recordings was 89% in Session 1 and 93% in Session 2.

3.2. ERP Results

3.2.1. Grand Average ERPs—C1: The peak of the first ERP component, C1, appeared 45–90 ms after stimulus onset. Figure 3a depicts the grand average ERP recorded at the Pz electrode for 20 subjects for Sessions 1 and 2. Effects of learning were assessed with an ANOVA with within-subject factors of session (1 and 2) and electrode site (CPz, Pz, POz). The C1 component is known to be most prominent in midline occipital and parietal electrodes (Pourtois et al., 2008; Qu et al., 2014), so hemisphere was not included as a factor in the ANOVAs for this component. Figure 3b shows C1 topographical maps at 70 ms following stimulus onset for Session 1 (left), Session 2 (middle), and their difference (Session 1–Session 2, right). TDT training resulted in a decreased (less negative) C1 amplitude over CPz, Pz and POz electrode sites ($F(1,57) = 11.58$, $p = 0.001$). There was no significant electrode by session interaction ($F(2,57) = 0.14$, $p = 0.86$). Next, we computed the magnitude of the effect of VPL on C1 amplitude by calculating the difference between Session 1 and Session 2 amplitude for each electrode (CPz, Pz and POz) and then averaging these difference scores. Furthermore, we defined the performance difference score as the difference in behavioral performance between Session 1 and Session 2. Across subjects, the effect of VPL on C1 amplitude was positively correlated with the performance difference score ($r = 0.456$, $p = 0.0497$; Figure 3c). There was not a significant main effect of Session on the latency of the C1 component, and there was no significant correlation between C1 latency difference and performance difference scores.

P1: Following C1, there was a positive ERP component (P1) between 80–130 ms. ANOVAs [session x electrode site (P1, Pz, P2) x hemisphere (ipsilateral, contralateral)] showed no significant effect of training on amplitude (main effect of session ($F(1,57) = 3.1$, $p = 0.08$), interaction between session and electrode ($F(2,57) = 0.24$, $p = 0.78$) and session and hemisphere ($F(1,38) = 0.95$, $p = 0.33$)) and/or latency of the P1 component (main effect of session ($F(1,57) = 0.57$, $p = 0.45$), interaction between session and electrode ($F(2,57) = 0.7$, $p = 0.49$) and session and hemisphere ($F(1,38) = 1.47$, $p = 0.23$)).

There was no correlation between P1 amplitude differences (Session 1–Session 2) and performance difference scores ($r = -0.02$, $p = 0.92$) and no significant correlation between P1 latency differences and performance difference score ($r = -0.27$, $p = -0.23$).

N1: The next visual evoked potential component, N1, was observed between 125–190 ms. Figure 4 shows the grand average ERPs at electrode PO3 (a) and topographical maps at 150 ms after stimulus onset for Session 1, Session 2, and their difference (Session 1–Session 2). (b) Training reduced N1 amplitude (Figure 4a, highlighted window). Results of the ANOVA [session x electrode site (P3, P5, P7, PO3, O1, P4, P6, P8, PO4, O2) x hemisphere] showed a significant main effect of session ($F(1,190) = 79.13$, $p < 0.001$) and no significant interaction between session and electrode ($F(9,190) = 1.62$, $p = 0.11$). N1 amplitude differences (Session 1–Session 2) were not significantly correlated with performance difference scores ($r = 0.19$, $p = 0.41$), and no significant interaction between session and hemisphere was observed for N1 amplitude ($F(1,38) = 0.02$, $p = 0.87$). There was a main effect of Session on N1 latency, with learning resulting in a faster N1 ($F(1,190) = 13.31$, $p < 0.001$), and no significant session x electrode interaction ($F(9,190) = 1.04$, $p = 0.41$). N1 latency differences associated with VPL were negatively correlated with performance difference scores ($r = -0.45$, $p = 0.046$) (Figure 4c). There was no significant interaction between session and hemisphere for N1 latency ($F(1,38) = 0.04$, $p = 0.82$).

P3: The P3 component was observed between 220–500 ms after stimulus onset (Figure 5a). ANOVA [session x electrode site (P1, Pz, P2) x hemisphere] revealed a significant increase in P3 amplitude in Session 2 ($F(1,57) = 42.94$, $p < 0.001$), with no significant session x electrode ($F(2,57) = 0.07$, $p = 0.93$) or session x hemisphere ($F(1,38) = 0.03$, $p = 0.85$) interaction. The increase in P3 amplitude with learning did not correlate with performance difference scores. There were no significant changes in P3 latency after training and no significant correlation between P3 latency differences and performance difference scores. No significant session x electrode ($F(2,57) = 0.36$, $p = 0.69$) or session x hemisphere ($F(1,38) = 0.41$, $p = 0.53$) interactions were observed for P3 latency.

To assess the relative contributions and independence of the decreases in C1 amplitude and N1 latency to improved behavioral performance following training, we conducted a stepwise linear regression analysis with C1 amplitude and N1 latency differences as independent variables and the performance difference score as the dependent variable. We found a statistically significant prediction of the performance difference score ($F(2,17) = 3.95$, $p = 0.039$; $r^2 = 0.32$) using these two predictors. In addition, N1 latency alone significantly predicted performance ($p = 0.046$), while C1 amplitude did not ($p = 0.11$). However,

including both predictors increased the overall model fit and variance explained (r-squared change = 0.114).

3.2.2. Latency-corrected Averages—The grand average ERP at electrode PO3 from Session 1 and its wavelet decomposition (traces in gray) are depicted in Figure 6a and b, respectively. Details in 6 levels (D1 to D6) contain the highest frequency components of the ERPs from D1 to the lower frequency components in D6, and the last approximation (A6) contains the lowest frequency components. Wavelet coefficients related to the ERP components were selected (Figure 6b, coefficients in red), and those not associated with evoked responses were set to zero (coefficients shown in gray) (see Methods). The denoised grand average signal (Figure 6a in red) was reconstructed using the selected coefficients. We used the same set of coefficients to denoise the average and single- trial ERPs for all subject at both sessions.

An example of an average ERP signal and ten single trials (traces in gray) are shown in Figure 6c and d, respectively. The red traces show the denoised trials, and the difference between the red and gray traces indicate the amount of background noise that was removed. The N1 peak latencies (local minimum between 125 to 190 ms after stimulus presentation; blue asterisks in Figure 6d) were estimated from the denoised single trials. The latency-corrected average (blue trace in Figure 6c) was obtained by aligning the N1 response latencies to that of the N1 response in the denoised average signal. As expected, this alignment resulted in larger N1 amplitudes. However, aligning to N1 added variability to C1, P1 and P3 latency estimates and decreased the amplitudes of these components (Figure 6c).

Figure 6e illustrates the grand average ERPs for both Session 1 (in solid blue) and Session 2 (solid red) and their latency-corrected grand averages (in dashed blue and dashed red, respectively). We applied the sign test to examine changes in amplitude following latency correction and found significantly increased N1 amplitude in both sessions ($p < 0.001$) but no increase in C1, P1, or P3 component amplitudes (Session 1: $p = 0.94$, $p = 0.59$, and $p = 0.97$, respectively; Session 2: $p = 0.99$, $p = 0.58$, and $p = 0.94$). These results reveal that changes in the N1 component are not necessarily accompanied by changes in C1, P1, or P3 components. Aligning to C1 latencies produced similar results: C1 amplitude was significantly increased (negatively) in both sessions ($p < 0.001$), while P1, N1 and P3 exhibited no significant increase (Session 1, P1: $p = 0.59$, N1: $p = 0.99$, P3: $p = 1$; Session 2, P1: $p = 0.94$, N1: $p = 0.99$, P3: $p = 0.99$). Note that for both C1 and N1 latency corrections we performed the latency corrected analysis on parietal and occipital electrode sites where we have clear observation of all four ERP components (C1,P1,N1,P3).

4. Discussion

The main goal of this study was to compare changes in early versus late cortical processing associated with VPL. We found significant changes in both early and late ERP components following TDT training, suggesting that the locus of neural plasticity associated with VPL is not exclusively early or late, but instead occurs across all tested levels of visual processing.

Specificity of VPL for stimulus features such as orientation and retinal location led early researchers to attribute learning to neural plasticity in early visual cortex (V1) (Ahissar and Hochstein, 1997; Karni and Sagi, 1991, 1993; Schoups et al., 1995), where neurons are highly selective for orientation and location. However, using different training procedures, many studies have demonstrated partial or complete transfer of VPL to stimuli with untrained orientations and locations (Wang et al., 2013; Zhang et al., 2015), suggesting contributions from higher-level cortical areas.

Previous ERP studies have attributed VPL of TDT to plasticity in primary visual cortex (V1) (Pourtois et al., 2008), changes in higher-level visual cortex (Qu et al., 2014), or changes in regions responsible for cognitive processes such as attention and decision-making (Wang et al., 2016). In this study, we demonstrated changes in scalp EEG signals following VPL that were associated with activity in both primary visual cortex (C1 component) and higher visual areas (N1) that are modulated by processes such as attention and target discrimination.

Although two recent ERP studies reported no changes in C1 amplitude following TDT learning (Qu et al., 2014; Wang et al., 2016), we found a significant decrease in the amplitude of C1 that is consistent with the ERP study of Pourtois et al. (2008). We also found a positive correlation between the magnitude of the change in C1 amplitude and improvement in behavioral performance. Previous single-unit recording studies in awake behaving monkeys (Li et al., 2004, 2008), as well as fMRI studies (Schwartz et al., 2002; Walker et al., 2005; Yotsumoto et al., 2008), also demonstrated changes in early visual cortex due to VPL. In addition, Bao and colleagues (2010) reported an increase in C1 amplitude that was accompanied by 30% improvement in performance in a contrast detection task following one month of training, although the ERPs used to assess physiological correlates of learning were recorded during performance of a central fixation task that directed attention away from the training stimuli. In contrast, Zhang et al. (2015) attributed the VPL-induced increases in C1 amplitude observed in their study to task-specific top-down modulation of C1.

The reduced C1 amplitude that we observed after TDT learning may be explained by changes in interactions between responses to the target and background elements. Responses of V1 neurons can be suppressed by contextual inputs outside but near their excitatory receptive fields (reviewed in Angelucci et al., 2017). In our study, the ERPs in response to the stimulus array reflect both the target and background elements, and there are many more background elements that cover a much larger portion of the visual field than the three target elements. TDT learning could therefore have enhanced suppression of the response to the background elements, thereby resulting in a decrease in C1 amplitude.

This C1 amplitude reduction could be due to top-down modulation of early visual cortex. Some studies have found that the amplitudes of P1 and N1, but not C1, are modulated by spatial attention (Di Russo, Martinez and Hilyard, 2003, Fu et al., 2001; Martinez et al., 1999). In contrast, recent studies reported top-down modulation of C1 amplitude by spatial attention (Kelly et al., 2008), affective evaluation (Pourtois et al., 2004; Stolarova, Keil and Moratti, 2006), and perceptual learning (Zhang et al., 2015). In the latter study, training on

an orientation discrimination task in one location increased the amplitude of C1 for stimuli at an untrained location that exhibited significant transfer of a behavioral measure of learning, consistent with top-down modulation due to high-level perceptual learning rather than plasticity in early visual cortex itself.

We also found a significant decrease in N1 amplitude following VPL, consistent with the results of Song et al. (2005), as well as a reduction in N1 latency that was negatively correlated with changes in behavioral performance. One interpretation of the decreased N1 latency is that texture discrimination becomes easier for the subjects after VPL, as N1 latency has been shown to be proportional to stimulus complexity (Ritter, Simson and Vaughan, 1983) and processing effort (Callaway & Halliday, 1982). Furthermore, perceptual learning of face processing significantly decreased N170 latency to the trained face compared with untrained faces (Su et al., 2012). In addition to these effects of task difficulty on N1 latency, there are analogous effects on N1 amplitude. Haider et al. (1964) showed that the N1 amplitude reflects the level of attention - as attention decreases, the N1 amplitude decreases. In addition, N1 amplitude is larger when subjects performed a discrimination task (color and/or letter discrimination of individual letters in an array) compared with a control condition in which subjects did not perform any discrimination and simply responded at the onset of any letter array (Vogel and Luck, 2000). A larger N1 amplitude due to task demands was also observed in combined magnetoencephalography (MEG) and ERP recordings (Hope et al., 2002). Finally, Fort et al. (2005) showed that the N1 component was larger in amplitude for an identification task compared with a simple detection task. From these studies, we may conclude that TDT learning makes the discrimination task easier and more automatic, so participants could complete the task with fewer attentional resources during Session 2 compared with Session 1.

Sleep facilitates consolidation of perceptual learning of the TDT task (Mednick et al., 2003; Stickgold, James and Hobson, 2000), with more improvement observed after a second night of sleep (48–96 hours after initial training) compared to one night of sleep. Sleep may also be necessary to elicit changes in ERP components with training. Atienza and Cantero (2001) found no training-related changes in latency of mismatch negativity (MMN) after a period of wakefulness, whereas MMN latency decreased during rapid eye movement (REM) sleep. These findings, along with those of Stickgold et al. (2000), may explain why we observed a decrease in N1 latency following VPL after two nights of sleep (see also Song et al. (2005)), while Pourtois et al. (2008), who examined effects of TDT learning the day after the end of training did not (Pourtois et al., 2008).

Finally, we found that VPL increased the amplitude of the P3 component, again consistent with the findings of Song et al. (2005). In our study, P3 amplitude enhancement was not correlated with improvements in behavioral performance.

Our finding of decreased amplitude of negative components C1 and N1 and increased amplitude of the positive P3 component following VPL raises the question of whether modulation of earlier components is simply propagated to the later components. We addressed this issue by latency correcting ERP averages for each of these components in each session. We found that alignment based on N1 latencies increased the amplitude of N1

but not the earlier C1 and P1 or the later P3 components. Analogous results were obtained when alignment was performed on C1 latencies. These findings suggest that the components we have studied are not part of the same neural generator and that, at the single-trial level, changes in one do not directly cause or reflect changes in the others.

5. Conclusion

In conclusion, our ERP study revealed neural changes in both early and later visual cortex following VPL of the TDT task. Specifically, we showed a significant decrease in C1 amplitude, indicating involvement of early visual cortex in a VPL task [replicating Pourtois et al., (2008)]. Moreover, we showed a significant correlation between this C1 decrease and behavioral differences following TDT learning. We also showed significant decreases in N1 amplitude and latency, indicating involvement of higher order cortical processes, as well as an increase in P3 amplitude. Furthermore, we showed a significant correlation between decreases in N1 latency and TDT behavioral differences.

Acknowledgments

This work was supported by the National Science Foundation (NSF) [BCS1439210], National Eye Institute Core Grant [EY003176], and NSF Graduate Research Fellowship Program.

References

Ahissar M, Hochstein S. Task difficulty and the specificity of perceptual learning. Nature. 1997; 387:401–406. [PubMed: 9163425]

Ahmadi M, Quian Quiroga R. Automatic denoising of single-trial evoked potentials. Neuroimage. 2013; 66:672–680. [PubMed: 23142653]

Angelucci A, Bijanzadeh M, Nurminen L, Federer F, Merlin S, Bressloff PC. Circuits and mechanisms for surround modulation in visual cortex. Annu Rev Neurosci. 2017; 40:425–451. [PubMed: 28471714]

Atienza M, Cantero JL. Complex sound processing during human REM sleep by recovering information from long-term memory as revealed by the mismatch negativity (MMN). Brain Res. 2001; 901:151–160. [PubMed: 11368962]

Bao M, Yang L, Rios C, He B, Engel SA. Perceptual learning increases the strength of the earliest signals in visual cortex. J Neurosci. 2010; 10:15080–15084.

Brainard DH. The psychophysics toolbox. Spat Vis. 1997; 10:433–436. [PubMed: 9176952]

Callaway E, Halliday R. The effect of attentional effort on visual evoked potential N1 latency. Psychiatry Res. 1982; 7:299–308. [PubMed: 6962438]

Clark VP, Fan S, Hillyard SA. Identification of early visual evoked potential generators by retinotopic and topographic analyses. Hum Brain Mapp. 1995; 2:170–187.

Conover WJ. Practical nonparametric statistics. 3. Vol. Chapter 3.4. Wiley; 1999. The sign test; 157–176.

Di Russo F, Martínez A, Sereno MI, Pitzalis S, Hillyard SA. Cortical sources of the early components of the visual evoked potential. Hum Brain Mapp. 2002; 15:95–111. [PubMed: 11835601]

Di Russo F, Martinez A, Hillyard SA. Source analysis of event-related cortical activity during visuo-spatial attention. Cereb Cortex. 2003; 13:486–499. [PubMed: 12679295]

Dosher BA, Lu ZL. Perceptual learning reflects external noise filtering and internal noise reduction through channel reweighting. Proc Natl Acad Sci. 1998; 95:13988–13993. [PubMed: 9811913]

Fort A, Besle J, Giard M, Pernier J. Task-dependent activation latency in human visual extrastriate cortex. Neurosci Lett. 2005; 379:144–148. [PubMed: 15823432]

Fu S, Fan S, Chen L, Zhuo Y. The attentional effects of peripheral cueing as revealed by two event-related potential studies. Clin Neurophysiol. 2001; 112:172–185. [PubMed: 11137676]

Furmanski CS, Schluppeck D, Engel SA. Learning strengthens the response of primary visual cortex to simple patterns. Curr Biol. 2004; 14:573–578. [PubMed: 15062097]

Haider M, Spong P, Lindsley DB. Attention, vigilance, and cortical evoked-potentials in humans. Science. 1964; 145:180–182. [PubMed: 14171563]

Hillyard SA, Anllo-Vento L. Event-related brain potentials in the study of visual selective attention. Proc Natl Acad Sci. 1998; 95:781–787. [PubMed: 9448241]

Hruby T, Marsalek P. Event-related potentials-the P3 wave. Acta Neurobiol Exp. 2002; 63:55–63.

Hung SC, Seitz AR. Prolonged training at threshold promotes robust retinotopic specificity in perceptual learning. J Neurosci. 2014; 34:8423–8431. [PubMed: 24948798]

Jasper H. Report of the committee on methods of clinical examination in electroencephalography. Electroencephalogr Clin Neurophysiol. 1958; 10:370–375.

Jeffreys D, Axford J. Source locations of pattern-specific components of human visual evoked potentials. I. component of striate cortical origin. Exp Brain Res. 1972; 16:1–21. [PubMed: 4646539]

Karni A, Sagi D. Where practice makes perfect in texture discrimination: Evidence for primary visual cortex plasticity. Proc Natl Acad Sci. 1991; 88:4966–4970. [PubMed: 2052578]

Karni A, Sagi D. The time course of learning a visual skill. Nature. 1993; 365:250–252. [PubMed: 8371779]

Kelly SP, Gomez-Ramirez M, Foxe JJ. Spatial attention modulates initial afferent activity in human primary visual cortex. Cereb Cortex. 2008; 18:2629–2636. [PubMed: 18321874]

Kleiner M, Brainard D, Pelli D, Ingling A, Murray R, Broussard C. What's new in Psychtoolbox-3? Perception. 2007; 36:1–16.

Li W, Piëch V, Gilbert CD. Perceptual learning and top-down influences in primary visual cortex. Nat Neurosci. 2004; 7:651–657. [PubMed: 15156149]

Li W, Piëch V, Gilbert CD. Learning to link visual contours. Neuron. 2008; 57:442–451. [PubMed: 18255036]

Linden DE. The p300: Where in the brain is it produced and what does it tell us? Neuroscientist. 2005; 11:563–576. [PubMed: 16282597]

Luck SJ, Woodman GF, Vogel EK. Event-related potential studies of attention. Trends Cogn Sci. 2000; 4:432–440. [PubMed: 11058821]

Luck SJ, Hillyard SA, Mouloua M, Woldorff MG, Clark VP, Hawkins HL. Effects of spatial cuing on luminance detectability: Psychophysical and electrophysiological evidence for early selection. J Exp Psychol: Hum Percept Perform. 1994; 20:887. [PubMed: 8083642]

Luck SJ, Heinze H, Mangun GR, Hillyard SA. Visual event-related potentials index focused attention within bilateral stimulus arrays. II. functional dissociation of P1 and N1 components. Electroencephalogr Clin Neurophysiol. 1990; 75:528–542. [PubMed: 1693897]

Mangun GR. Neural mechanisms of visual selective attention. Psychophysiology. 1995; 32:4–18. [PubMed: 7878167]

Martinez A, Anllo-Vento L, Sereno MI, Frank LR, Buxton RB, Dubowitz D, Wong EC, Hinrichs H, Heinze HJ, Hillyard SA. Involvement of striate and extrastriate visual cortical areas in spatial attention. Nat Neurosci. 1999; 2:364–369. [PubMed: 10204544]

Mednick S, Nakayama K, Stickgold R. Sleep-dependent learning: A nap is as good as a night. Nat Neurosci. 2003; 6:697–698. [PubMed: 12819785]

Navajas J, Ahmadi M, Quian Quiroga R. Uncovering the mechanisms of conscious face perception: A single-trial study of the n170 responses. J Neurosci. 2013; 33:1337–1343. [PubMed: 23345210]

Noesselt T, Hillyard SA, Woldorff MG, Schoenfeld A, Hagner T, Jäncke L, Tempelmann C, Hinrichs H, Heinze H. Delayed striate cortical activation during spatial attention. Neuron. 2002; 35:575–587. [PubMed: 12165478]

Pelli DG. The VideoToolbox software for visual psychophysics: Transforming numbers into movies. Spat Vis. 1997; 10:437–442. [PubMed: 9176953]

Petrov AA, Dosher BA, Lu Z. The dynamics of perceptual learning: An incremental reweighting model. Psychol Rev. 2005; 112:715. [PubMed: 16262466]

Polich J. Updating P300: An integrative theory of P3a and P3b. Clin Neurophysiol. 2007; 118:2128–2148. [PubMed: 17573239]

Polich J, Kok A. Cognitive and biological determinants of P300: An integrative review. Biol Psychol. 1995; 41:103–146. [PubMed: 8534788]

Pourtois G, Rauss KS, Vuilleumier P, Schwartz S. Effects of perceptual learning on primary visual cortex activity in humans. Vision Res. 2008; 48:55–62. [PubMed: 18082238]

Pourtois G, Grandjean D, Sander D, Vuilleumier P. Electrophysiological correlates of rapid spatial orienting towards fearful faces. Cereb Cortex. 2004; 14:619–633. [PubMed: 15054077]

Qu Z, Wang Y, Zhen Y, Hu L, Song Y, Ding Y. Brain mechanisms underlying behavioral specificity and generalization of short-term texture discrimination learning. Vision Res. 2014; 105:166–176. [PubMed: 25449163]

Quian Quiroga R, Atienza M, Cntero JL, Jongsma MLA. What can we learn from single-trial event-related potentials? Chaos Complex Lett. 2007; 2:345–363.

Quian Quiroga R. Obtaining single stimulus evoked potentials with wavelet denoising. Phys D Nonlinear Phenom. 2000; 145:278–292.

Quian Quiroga R, Garcia H. Single-trial event-related potentials with wavelet denoising. Clin Neurophysiol. 2003; 114:376–390. [PubMed: 12559247]

Raiguel S, Vogels R, Mysore SG, Orban GA. Learning to see the difference specifically alters the most informative V4 neurons. J Neurosci. 2006; 26:6589–6602. [PubMed: 16775147]

Rey HG, Ahmadi M, Quiroga RQ. Single trial analysis of field potentials in perception, learning and memory. Curr Opin Neurobiol. 2015; 31:148–155. [PubMed: 25460071]

Ritter W, Simson R, Vaughan HG. Event-related potential correlates of two stages of information processing in physical and semantic discrimination tasks. Psychophysiology. 1983; 20:168–179. [PubMed: 6844516]

Rugg M, Milner A, Lines C, Phalp R. Modulation of visual event-related potentials by spatial and non-spatial visual selective attention. Neuropsychologia. 1987; 25:85–96. [PubMed: 3574653]

Schoups AA, Vogels R, Orban GA. Human perceptual learning in identifying the oblique orientation: Retinotopy, orientation specificity and monocularity. J Physiol. 1995; 483(Pt 3):797–810. [PubMed: 7776259]

Schwartz S, Maquet P, Frith C. Neural correlates of perceptual learning: A functional MRI study of visual texture discrimination. Proc Natl Acad Sci. 2002; 99:17137–17142. [PubMed: 12446842]

Seitz A, Watanabe T. A unified model for perceptual learning. Trends Cogn Sci. 2005; 9:329–334. [PubMed: 15955722]

Sigman M, Pan H, Yang Y, Stern E, Silbersweig D, Gilbert CD. Top-down reorganization of activity in the visual pathway after learning a shape identification task. Neuron. 2005; 46:823–835. [PubMed: 15924867]

Song Y, Ding Y, Fan S, Qu Z, Xu L, Lu C, Peng D. Neural substrates of visual perceptual learning of simple and complex stimuli. Clin Neurophysiol. 2005; 116:632–639. [PubMed: 15721077]

Stickgold R, James L, Hobson A. Visual discrimination learning requires sleep after training. Nat Neurosci. 2000; 3:1237–1238. [PubMed: 11100141]

Stolarova M, Keil A, Moratti S. Modulation of the C1 visual event-related component by conditioned stimuli: Evidence for sensory plasticity in early affective perception. Cereb Cortex. 2006; 16:876–887. [PubMed: 16151178]

Su J, Chen C, He D, Fang F. Effects of face view discrimination learning on N170 latency and amplitude. Vision Res. 2012; 61:125–131. [PubMed: 21911001]

Sutton S, Braren M, Zubin J, John ER. Evoked-potential correlates of stimulus uncertainty. Science. 1965; 150:1187–1188. [PubMed: 5852977]

Van Voorhis S, Hillyard SA. Visual evoked potentials and selective attention to points in space. Percept Psychophys. 1977; 22:54–62.

Vogel EK, Luck SJ. The visual N1 component as an index of a discrimination process. Psychophysiology. 2000; 37:190–203. [PubMed: 10731769]

Walker MP, Stickgold R, Jolesz FA, Yoo SS. The functional anatomy of sleep-dependent visual skill learning. Cereb Cortex. 2005; 15:1666–1675. [PubMed: 15703253]

Wang F, Huang J, Lv Y, Ma X, Yang B, Wang E, Du B, Li W, Song Y. Predicting perceptual learning from higher-order cortical processing. Neuroimage. 2016; 124:682–692. [PubMed: 26391126]

Wang R, Cong L, Yu C. The classical TDT perceptual learning is mostly temporal learning. J Vision. 2013; 13(5):9–9. 1–9.

Yotsumoto Y, Watanabe T, Sasaki Y. Different dynamics of performance and brain activation in the time course of perceptual learning. Neuron. 2008; 57:827–833. [PubMed: 18367084]

Zhang G, Li H, Song Y, Yu C. ERP C1 is top-down modulated by orientation perceptual learning. J Vision. 2015; 15(10):8–11. 1–11.

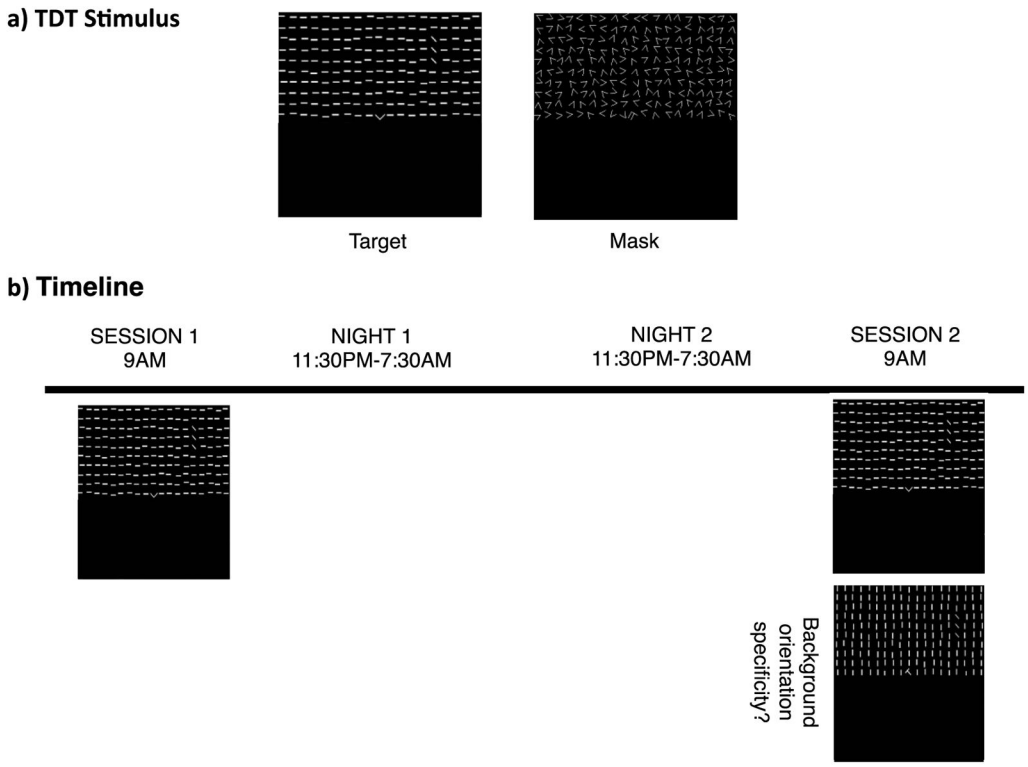

Figure 1.

Stimuli and experimental timeline. (a) Left panel: the texture stimulus consisted of a fixation letter (T or L, central target) and a set of three diagonal bars, arranged either vertically or horizontally (peripheral target; in this example, presented in the upper right visual field), embedded within a background of horizontally-oriented elements. Participants were asked to report the identity of the fixation letter and the target orientation. Right panel: the mask consisted of randomly oriented V-shaped elements with a superimposed L or T (also with random orientation) at the fixation point. (b) Session 1 started at 9 AM on Day 1 with two runs of the TDT: one with constant ISI (used for ERP analysis), and one with a progressively decreasing ISI (used for estimating behavioral thresholds). Session 2 started at 9 AM on Day 3 (48 hours after the first session, following two full days of wake and two full nights of sleep), with three TDT runs: one for ERP analysis, and one each for estimating behavioral thresholds for trained and untrained background orientations.

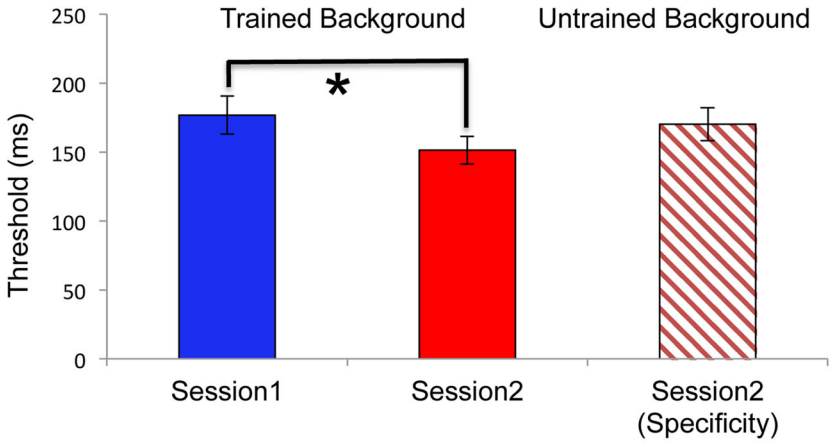

Figure 2.

Behavioral thresholds. The trained background threshold was significantly lower in Session 2 compared to Session 1, indicating performance improvements after TDT training. In addition, the untrained threshold in Session 2 was not significantly different from the Session 1 threshold, but it was significantly greater than the trained background in Session 2, indicating that learning did not transfer to an untrained background orientation. Error bars are standard errors of the mean across subjects.

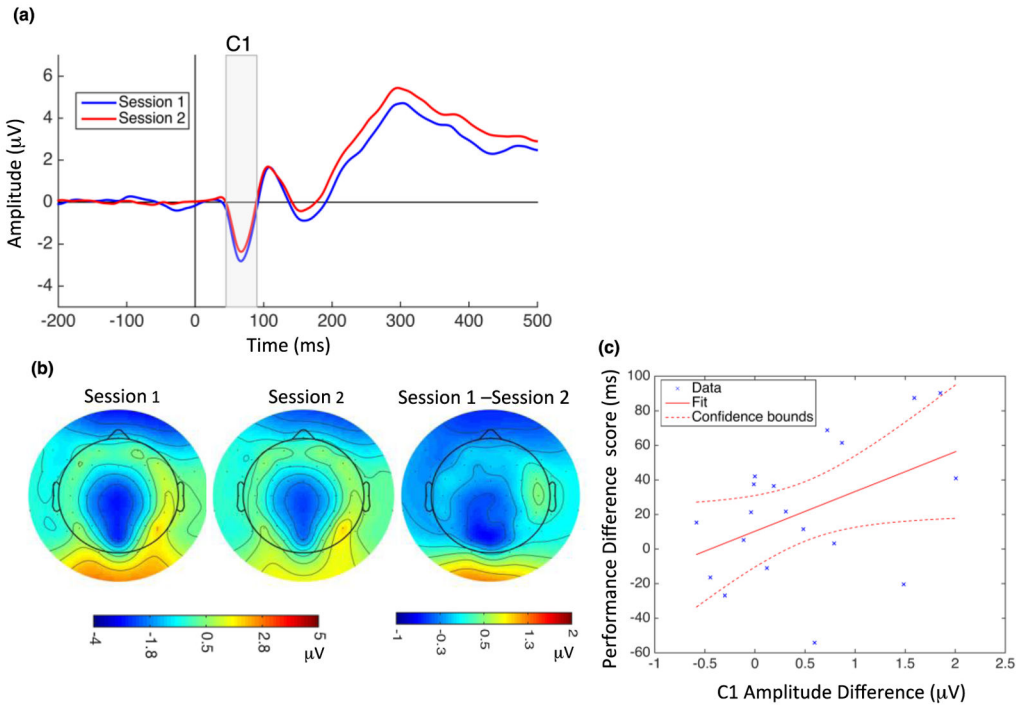

Figure 3.

Modulation of C1 amplitude by perceptual learning and correlation with behavioral changes. (a) Grand average ERPs recorded at Pz electrode site during Session 1 (blue) and Session 2 (red). Vertical line at zero indicates the onset of the TDT target array, and the gray highlighted rectangle indicates the temporal window used for C1 analysis. C1 amplitude significantly decreased following learning (mean C1 amplitude in Session 1: −1.80 μV, SD = 1.52; Session 2: −1.36 μV, SD = 1.45). (b) C1 topographical map at 70 ms after stimulus onset for Session 1 (left), Session 2 (middle), and their difference (right). (C) C1 amplitude changes and performance difference scores were significantly correlated. Dotted lines indicate 95% confidence interval.

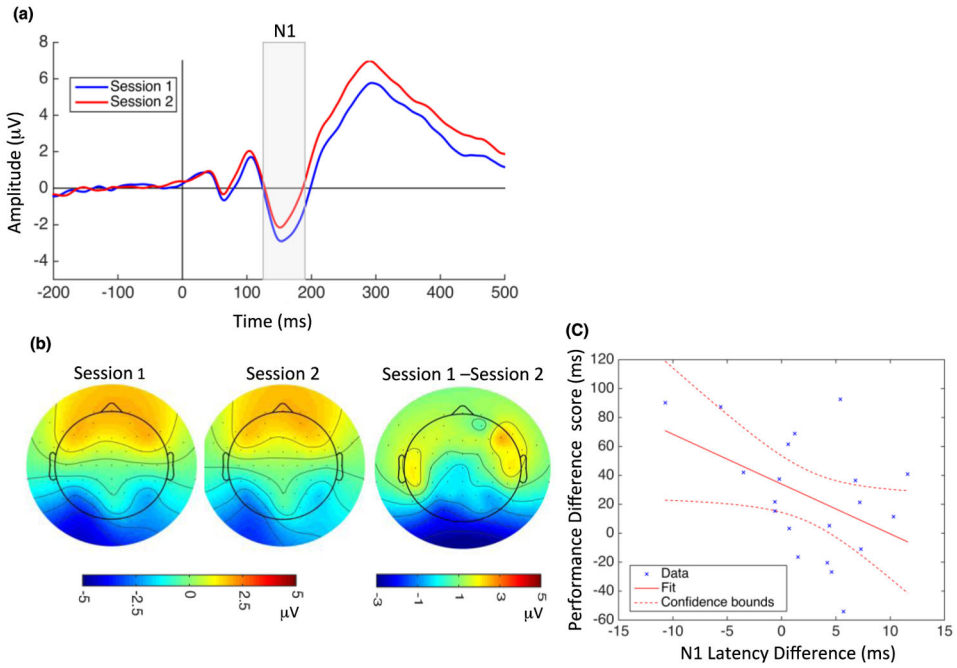

Figure 4.

Modulation of N1 amplitude and latency by perceptual learning and correlation with behavioral changes. (a) Grand average ERPs recorded at PO3 electrode during Session 1 (blue) and Session 2 (red). Vertical line at zero indicates the onset of TDT target array presentation, and the gray highlighted rectangle indicates the temporal window used for N1 analysis. Both N1 amplitude (mean N1 in Session 1: −2.04 μV, SD = 2.89; Session 2: −1.15 μV, SD = 2.75) and latency (Session 1: 159 ms, SD = 17.5; Session 2: 155 ms, SD = 19.4) decreased significantly following learning. (b) N1 topographical map 150 ms after stimulus onset for Session 1 (left), Session 2 (middle), and their difference (right). (c) N1 latency changes were negatively correlated with performance difference scores. Dotted lines indicate 95% confidence interval.

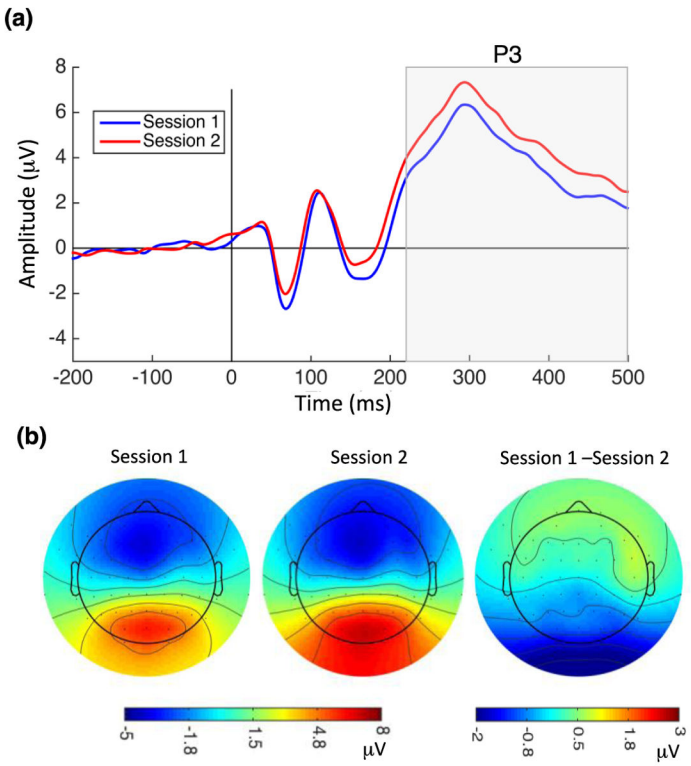

Figure 5.

Perceptual learning increased P3 amplitude. (a) Grand average ERPs recorded at POz electrode for Session 1 (blue) and Session 2 (red). Vertical line at zero indicates the onset of TDT target array presentation, and the gray highlighted rectangle indicates the temporal window used for P3 analysis. P3 amplitude increased significantly following learning (mean P3 in Session 1: 3.89 μV, SD = 2.36; Session 2: 4.83 μV, SD = 2.53). (b) P3 topographical map 300 ms after stimulus onset for Session 1 (left), Session 2 (middle), and their difference (right).

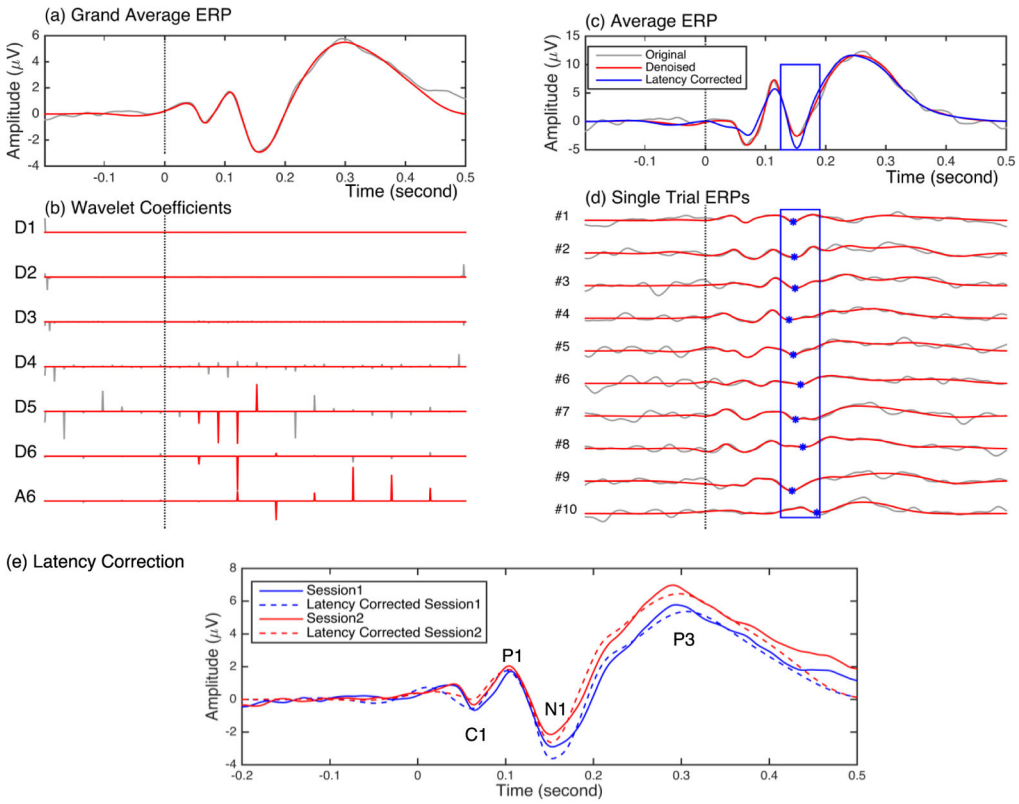

Figure 6.

Wavelet denoising and latency-corrected averaging. (a) Original (gray) and denoised (red) grand average ERPs from electrode PO3. (b) Six-scale wavelet decomposition of the original grand average ERPs (gray) and denoised coefficients (red). Vertical dotted lines represent stimulus onset time. The denoised grand average ERPs (in red) were reconstructed using the selected wavelet coefficients (in red). (c) An example average ERP and (d) its first ten single trials (gray). Red traces shows denoised (see Methods) time series for the average (c) and for single trials (d). Asterisks indicate the N1 peaks in each single trial, and the blue rectangle shows the N1 analysis window. Latency-corrected averages (blue) were obtained by temporally aligning single-trial N1 components to the N1 component of the denoised average ERP. (e) Original (solid traces) and N1 latency-corrected (dashed traces) grand averages for Session 1 (blue) and Session 2 (red). Latency correction to N1 increased the amplitude of the N1 component but not those of the C1, P1 or P3 components.